optica

Fluctuations and noise-limited sensing near the exceptional point of parity-time-symmetric resonator systems

N. Asger Mortensen,[1,2,3,*] P. A. D. Gonçalves,[1,3,4] Mercedeh Khajavikhan,[5] Demetrios N. Christodoulides,[5] Christos Tserkezis,[1] and Christian Wolff[1]

[1]Center for Nano Optics, University of Southern Denmark, Campusvej 55, DK-5230 Odense M, Denmark
[2]Danish Institute for Advanced Study, University of Southern Denmark, Campusvej 55, DK-5230 Odense M, Denmark
[3]Center for Nanostructured Graphene, Technical University of Denmark, DK-2800 Kongens Lyngby, Denmark
[4]Department of Photonics Engineering, Technical University of Denmark, DK-2800 Kongens Lyngby, Denmark
[5]CREOL/College of Optics and Photonics, University of Central Florida, Orlando, Florida 32816, USA
*Corresponding author: asger@mailaps.org

Exceptional points of parity-time ($\mathcal{PT}$) symmetric systems hold an intriguing potential for highly sensitive sensors. Here, we theoretically explore the role of mesoscopic fluctuations and noise on the spectral and temporal properties of systems of $\mathcal{PT}$-symmetric-coupled gain–loss resonators operating near the exceptional point, where eigenvalues and eigenvectors coalesce. We show that experimentally inevitable detuning in the frequencies of the uncoupled resonators leads to an unavoidable modification of the conditions for reaching the exceptional point, while, as this point is approached in ensembles of resonator pairs, statistical averaging significantly smears the spectral features. We discuss how these fluctuations affect the sensitivity of sensors based on coupled $\mathcal{PT}$-symmetric resonators. Finally, we show that temporal fluctuations in the detuning and gain of these sensors lead to at least a quadratic growth of the optical power in time, implying that maintaining operation at the exceptional point over a long period can be rather challenging. Our theoretical analysis clarifies issues central to the realization of $\mathcal{PT}$-symmetric devices, and should facilitate future experimental work in the field.   © 2018 Optical Society of America under the terms of the OSA Open Access Publishing Agreement

https://doi.org/10.1364/OPTICA.5.001342

1. INTRODUCTION

Pronounced sample-to-sample fluctuations constitute a hallmark of mesoscopic physics [1], where the finite number of degrees of freedom limits the self-averaging common to macroscopic systems. In mesoscopic systems, the interactions of waves with disordered potentials lead to many fascinating phenomena [2], including Anderson localization [3], weak localization [4], and universal conductance fluctuations [5]. A typical playground for such effects is many-body electron physics, which is rich in mesoscopic fluctuations [6–9]. Another class of interesting systems can be found in optics, with intriguing examples including random lasers [10] and quantum optical entanglement in multiple-scattering media [11], as well as cavity-quantum electrodynamics [12] and nanolasing [13] with Anderson localized states. Traditionally, many mesoscopic wave-interference phenomena have been explored using the tight-binding model of condensed-matter physics [14], while its optical analog—coupled-mode theory (CMT) [15]—has fostered the exploration of systems consisting of coupled resonators, with an emphasis on long chains (waveguides) [16], and the rich interplay of slow-light phenomena

with the presence of both loss and gain [17] as well as disorder-induced Anderson localization [18]. While the quantum dynamics is commonly governed by Hermitian equations of motion, the electrodynamics of optical systems is in general non-Hermitian due to the inevitable presence of material absorption, but also the possibility of introducing optical gain. However, recent years have witnessed not only efforts to realize loss compensation in optical metamaterials [19], but also the possibility to enable parity-time ($\mathcal{PT}$)-symmetric systems [20,21], where eigenvalues can be real despite the non-Hermitian aspects of the governing equations [22].

2. MODEL

Here, we turn to finite $\mathcal{PT}$-symmetric systems and illustrate interesting new mesoscopic fluctuations of the spectral properties near the exceptional point (EP) with coalescing eigenstates. For the transparency of our illustration, we consider a problem of two coupled resonators, as illustrated in Fig. 1. Within CMT, the dynamics is governed by a Schrödinger-like equation:
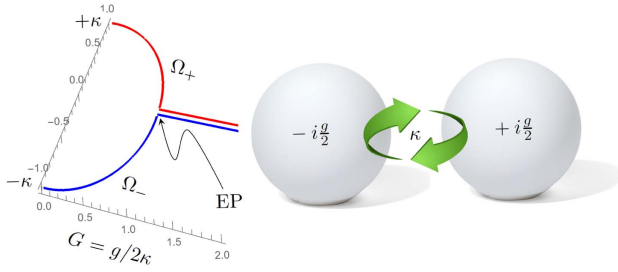
Fig. 1. Schematic illustration of a $\mathcal{PT}$-symmetric dimer formed by two identical (no frequency detuning) coupled optical resonators, but with opposite values of the gain–loss parameter $G(\equiv g/2\kappa)$. In the absence of gain–loss ($G = 0$), the two resonators form common hybridized states with splitting by 2κ, while for the exceptional point (EP) at $G = 1$, the system is degenerate, i.e., $\Omega_+ = \Omega_-$, with coalescing eigenstates.

$$i\partial_t \underbrace{\begin{pmatrix} a(t) \\ b(t) \end{pmatrix}}_{\psi(t)} = \underbrace{\begin{pmatrix} \omega_a - i\frac{g}{2} & \kappa \\ \kappa & \omega_b + i\frac{g}{2} \end{pmatrix}}_{\mathcal{H}} \begin{pmatrix} a(t) \\ b(t) \end{pmatrix}, \qquad (1)$$

where ω_a, ω_b, a, and b are the resonance frequencies of the uncoupled resonators and the amplitudes of their respective modes, κ is the coupling parameter (which can be chosen real-valued), and g characterizes the gain and damping of the two resonators. For convenience, we have introduced symbols $\psi(t)$ and $\mathcal{H}$ for the state and the Hamiltonian, respectively. In the analysis of such a problem, it is customary to study stationary solutions (we will come back to the time evolution toward the end of this paper), i.e., the eigenvalue problem $\mathcal{H}\psi = \omega\psi$. For $g = 0$, this constitutes a Hermitian problem and corresponds to the usual hybridization of two levels, i.e., with the bonding and anti-bonding states (notation inherited from molecular orbital bonding theory) having real eigenfrequencies and, in the $\omega_a = \omega_b$ case, being separated by an energy of 2κ.

In the presence of a finite g, the system becomes non-Hermitian, while $\mathcal{PT}$-symmetry may still allow real-valued eigenfrequencies [22], depending on the strength of the gain g relative to the coupling κ. Perhaps the most notable characteristic of a $\mathcal{PT}$-symmetric system is a $\mathcal{PT}$-symmetry breaking transition that takes place around $g/2\kappa = 1$. In optical settings, this abrupt phase transition has been experimentally demonstrated in coupled waveguides and cavities, by measuring both the real and imaginary components of the eigenvalues, as well as by observing the evolution of the corresponding mode profile [23–28].

In order to analyze the influence of temporally fluctuating environments or sample-to-sample fluctuations associated with inevitable small variations in ω_a and ω_b, we shall in the following allow a small, but finite frequency detuning between the two coupled resonators. To ease our notation, we first define a normalized frequency $\Omega = \omega/\kappa$ and center frequency $\bar{\Omega} = (\omega_a + \omega_b)/2\kappa$, while the normalized detuning of the two resonances is denoted by $\Delta = (\omega_a - \omega_b)/2\kappa$. The eigenvalue problem $\mathcal{H}\psi = \omega\psi$ now takes the form

$$\begin{pmatrix} \bar{\Omega} + \Delta - iG & 1 \\ 1 & \bar{\Omega} - \Delta + iG \end{pmatrix}\begin{pmatrix} a \\ b \end{pmatrix} = \Omega \begin{pmatrix} a \\ b \end{pmatrix}, \qquad (2a)$$

where $G = g/2\kappa$ is the normalized parameter central to the analysis of EPs in this problem. By straightforward diagonalizing, we get

$$\Omega_\pm = \bar{\Omega} \pm \sqrt{1 - (G + i\Delta)^2}, \qquad (2b)$$

with corresponding eigenvectors

$$\psi_\pm = \begin{pmatrix} a \\ b \end{pmatrix}_\pm = \begin{pmatrix} -i(G + i\Delta) \pm \sqrt{1 - (G + i\Delta)^2} \\ 1 \end{pmatrix}. \qquad (2c)$$

Obviously, the eigenfrequencies of the coupled system can in general be complex, i.e., $\Omega = \Omega' + i\Omega''$, and we immediately see how detuning enters simply as an imaginary part of the gain parameter: $G^2 \rightarrow (G + i\Delta)^2$. Equations (2b) and (2c) nicely illustrate how both the eigenvalues and the eigenstates coalesce ($\Omega_+ = \Omega_-$ and $\psi_+ = \psi_-$) when the square root vanishes, forming an EP. If the two uncoupled resonators are perfectly aligned ($\Delta = 0$), this occurs for $G = 1$, where the gain and loss are exactly balanced by an appropriate coupling constant.

Under realistic experimental conditions, the inherent material loss can always be compensated by carefully adjusting the gain, e.g., through electrical pumping of one of the resonators [29]. However, no matter the efforts spent in fabricating resonators with similar resonance frequencies, there will always be some small, yet inevitable frequency detuning. Moreover, this detuning will vary from sample to sample. In a particular sample, the detuning is also likely to fluctuate over time due to unavoidable fluctuations in the environment. In this paper, we study the interplay of such sample-to-sample fluctuations and its behavior and magnitude near EPs. We also consider possible implications of fluctuating environments for the exploration of EPs in sensing [30]. While we here focus on fluctuations in Δ, it is clear from Eq. (2a) that fluctuations in G would have quite similar implications.

3. RESULTS

A. Below the Exceptional Point

For low gain ($G \ll 1$), we have to leading order in the detuning that the eigenvalues become

$$\Omega'_\pm \simeq \bar{\Omega} \pm \left(1 + \frac{1}{2}\Delta^2\right), \qquad (3a)$$

$$\Omega''_\pm \simeq \mp G\Delta. \qquad (3b)$$

In the ideal case ($\Delta = 0$), this regime is characterized by a real-valued spectrum, i.e., $\Omega = \bar{\Omega} \pm 1$. However, for a small, but finite detuning, the imaginary part is finite despite the symmetric gain–loss arrangement. In other words, the finite detuning breaks the $\mathcal{PT}$-symmetry associated with perfectly aligned resonators [20]. This is also immediately clear by noticing that the Hamiltonian does not equal its adjoint, i.e., $\mathcal{H} \neq \mathcal{H}^\dagger$.

B. Fluctuations Near the Exceptional Point

In order to see that detuning changes the conditions for having an EP, we expand the exact expression [Eq. (2b)] around the EP $G = 1$; to leading order in Δ, we get [31]

$$\Omega_\pm \simeq \bar{\Omega} \pm (1 - i)\sqrt{\Delta}. \qquad (4)$$

The detuning lifts the degeneracy that would otherwise be associated with the EP of two perfectly aligned resonators ($\Delta = 0$). Away from the EP, systems are commonly affected linearly by perturbation. However, the fact that the splitting scales as $\sqrt{\Delta}$ is an interesting manifestation of the system being very susceptible to perturbations near the EPs [32,33]. Obviously, this can be used to our advantage in the context of optical sensors [30], but has the
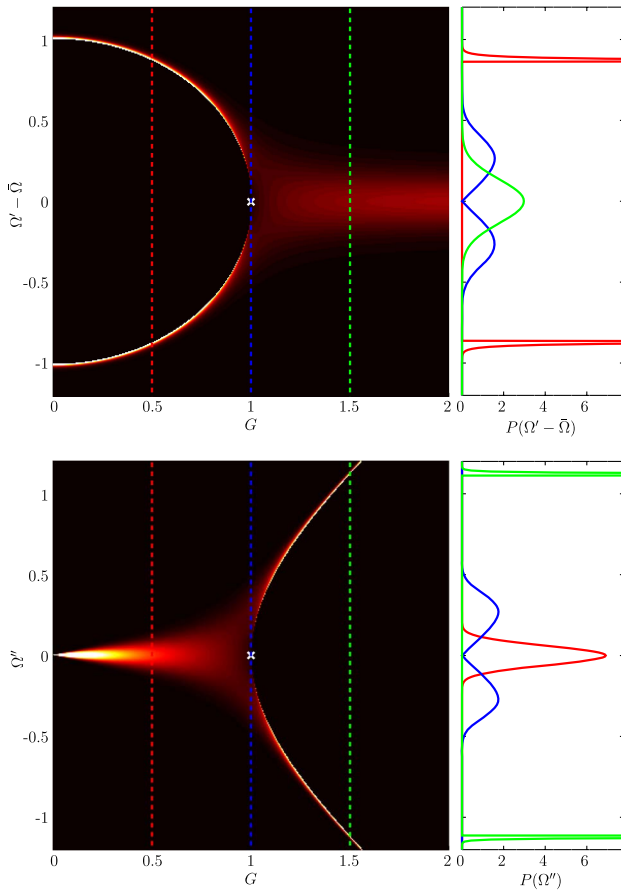
natural drawback that the system is also very sensitive to any undesired, yet practically inevitable degrees of freedom associated with fabrication imperfections or fluctuating environments (e.g., temperature shifts or noise in the gain parameter).

We now assume an ensemble of resonator pairs with a Gaussian distribution of the detuning parameter:

$$P_0(\Delta) = \frac{1}{\sqrt{2\pi}\sigma}\,\exp\left(-\frac{1}{2}\Delta^2/\sigma^2\right). \quad (5)$$

This can be interpreted either as fabrication tolerance or as temporal fluctuations assuming that an ergodic approximation to the system dynamics is valid. In order to appreciate the dramatic effect this has on the spectrum especially near the EP, we show in Fig. 2 the distribution of the real and imaginary parts of the eigenvalues, where the variance $\sigma = 0.1$ was chosen sufficiently small, so that the common regime with $G = 0$ is only slightly broadened. However, in the vicinity of the EP (and beyond), we observe a very pronounced smearing of the spectral features.

Pursuing a deeper understanding of this numerical observation, we proceed with analytical calculations based on the leading-order correction in Eq. (4). The eigenvalue Ω is not a convenient quantity to study at an isolated point of degeneracy that is lifted by a statistical process. Instead, we shall focus on the splitting of the eigenvalues' real part:

$$\Sigma = \Omega'_+ - \Omega'_- \approx 2\sqrt{|\Delta|}. \quad (6)$$

It should be noted that corresponding expressions for fluctuations in the gain coefficient and for the splitting of Ω'' are very similar. Its ensemble average is

$$\langle\Sigma\rangle = 2\int_{-\infty}^{\infty} d\Delta\,\sqrt{|\Delta|}P(\Delta) = 2^{5/4}\Gamma\left(\frac{3}{4}\right)\sqrt{\frac{\sigma}{\pi}} \approx 1.64\sqrt{\sigma}. \quad (7)$$

Given the Gaussian distribution of the detuning, the distribution of eigenfrequencies at the EP can now be evaluated:

$$P(\Omega') \simeq \frac{1}{\sqrt{\sigma}}F\left(\frac{\Omega'-\bar{\Omega}}{\sqrt{\sigma}}\right), \quad (8)$$

where $F(x) = (\frac{8}{\pi})^{1/2}|x|\exp(-\frac{1}{2}x^4)$. This approximate universal distribution shown in Fig. 3 illustrates an interesting ensemble-averaged broadening of levels inside the gap, i.e., a $P(\Omega') \propto |\Omega'-\bar{\Omega}|$ for energies smaller than the detuning. Within the square root scaling law, $P(\Omega'')$ is distributed in the same manner; the cuts through the EP (solid blue curves) of the two panels in Fig. 2 are nearly identical, but not quite, due to the finite σ.
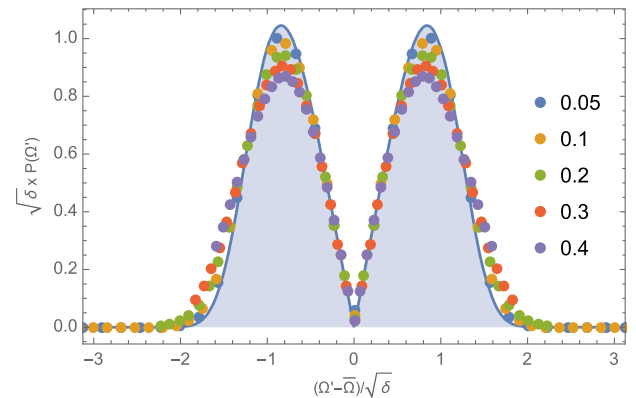
C. Sensitivity of Fluctuating Sensors

It is not entirely surprising that statistical detuning leads to a non-zero average eigenvalue splitting. The natural next question is how this affects the performance of a sensor, i.e., how the average splitting $\langle\Sigma\rangle$ reflects additional, non-fluctuating detuning. We now assume that this detuning parameter has two contributions: first a fluctuating detuning due to unintended noise, which is inevitably present in any realization of such systems, and second, the signal Δ_0 that is meant to be detected or sensed. For the detuning probability distribution

$$P(\Delta) = \frac{1}{\sqrt{2\pi}\sigma}\,\exp\left[-\frac{1}{2}(\Delta-\Delta_0)^2/\sigma^2\right], \quad (9)$$

the sensitivity of the time-averaged frequency splitting can now be written as

$$\frac{\partial\langle\Sigma\rangle}{\partial\Delta_0} = \sqrt{\frac{2}{\pi}}\sigma^{-1/2}\underbrace{\int_{-\infty}^{\infty} dx\,\sqrt{\left|x+\frac{\Delta_0}{\sigma}\right|}x\,\exp\left(-\frac{1}{2}x^2\right)}_{I(\Delta_0/\sigma)}. \quad (10)$$

Fig. 2. Plots of the distribution of complex eigenfrequencies $\Omega = \Omega' + i\Omega''$ for varying G. The upper panel shows $P(\Omega')$, while $P(\Omega'')$ is displayed in the lower panel for an ensemble of coupled resonators with $\sigma = 0.1$. Clearly, the sample-to-sample fluctuations are pronounced as one approaches the exceptional point. The right-hand panels show eigenfrequency distributions for specific values of $G = (0.5, 1, 1.5)$ corresponding to the dashed vertical lines in the left-hand panels.

Fig. 3. Plot of the distribution of $P(\Omega')$ versus $\Omega' - \bar{\Omega}$ at the exceptional point $(G = 1)$ for ensembles of coupled resonators with $\sigma = 0.05, 0.1, 0.2, 0.3,$ and 0.4. Data points are the results of numerical ensemble averaging of the spectra associated with Eq. (2b), while the filled curve shows the approximate universal result from Eq. (8).

Here, the integral can be approximated in small- and large-signal limits:

$$I(\Delta_0/\sigma) \approx \begin{cases} \frac{\Delta_0}{\sigma}, & \Delta_0 \ll \sigma \\ \sqrt{\frac{\pi}{2}}\sqrt{\frac{\sigma}{\Delta_0}}, & \Delta_0 \gg \sigma \end{cases}, \quad (11)$$

and in Fig. 4, we show these asymptotic behaviors (dashed lines) along with a full numerical evaluation of the integral (red line). The integral is always smaller than unity, implying that the sensitivity is noise limited, i.e., $\partial\langle\Sigma\rangle/\partial\Delta_0 < \sigma^{-1/2}$. The sensitivity should be contrasted to the case in the absence of fluctuations, where there is a tremendous sensitivity to small signals, i.e., $\partial\Sigma/\partial\Delta_0 = \Delta_0^{-1/2}$. Indeed, from Eq. (11), we recover this result for $\sigma \to 0$. On the other hand, it is quite clear how the sensitivity vanishes linearly in the low-signal limit, where the perturbation is dressed by the noise. While figures of merit are commonly adapted to quantify the performance of linearly responding sensors (see, e.g., [34,35]), the power-law response of EPs makes it impossible to directly adapt such a linear concept. To illustrate the constrained sensitivity due to noise, we here use the limiting case $(\sigma \to 0)$ to introduce the sensitivity-diminution factor $(\Delta_0^{1/2}\partial\langle\Sigma\rangle/\partial\Delta_0)$ shown in Fig. 4 (filled curve). There is a clear diminution of the sensitivity to perturbations for $\Delta_0 < \sigma$, while the noise-less sensing performance is recovered only for $\Delta_0 \gtrsim 2\sigma$.

D. Time Evolution

The use of EPs in highly sensitive sensors is seriously hampered by the low-frequency tail of the temporal fluctuations of detuning and gain. This tail is called drift and must be compensated by a feedback loop, i.e., the sensor is kept at the EP by constantly adjusting detuning and pump power, and the actually measured quantities are the values of these feedback variables (e.g., pump power for the gain or heating currents for the detuning). For this, it seems necessary to keep the sensor at the EP over an extended period of time. Naively, this seems trivial, because the eigenstate has a real eigenvalue, and one would therefore expect the time-evolution to be stationary and neither growing nor decaying in time. In reality, this is not the case.

At the EP, the equation of motion [Eq. (1)] reads

$$i\partial_\tau\psi = \mathcal{H}_0\psi; \qquad \mathcal{H}_0 = \begin{pmatrix} \bar{\Omega} - i & 1 \\ 1 & \bar{\Omega} + i \end{pmatrix}, \quad (12)$$
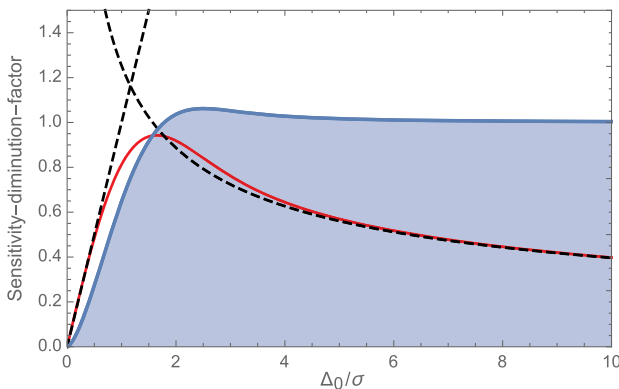
Fig. 4. Sensitivity-diminution factor (filled curve) versus Δ_0/σ, with σ representing the noise/fluctuations. The integral $I(\Delta_0/\sigma)$ in Eq. (10) is also shown (red line), along with the asymptotic behaviors in Eq. (11) indicated by dashed lines.

where $\tau = \kappa t$ is the dimensionless time variable. We can solve this formally using the time-evolution operator [36]:

$$\psi(\tau) = \mathcal{U}_0(\tau)\psi(0) = \exp(-i\mathcal{H}_0\tau)\psi(0). \quad (13)$$

The matrix exponential can be simplified by decomposing $\mathcal{H}_0 = \bar{\Omega}\mathbb{I} + A$, where $\mathbb{I}$ is the unit matrix, and $A = \begin{pmatrix} -i & 1 \\ 1 & i \end{pmatrix}$. Since $\mathbb{I}$ and A commute, we find

$$\mathcal{U}(\tau) = \exp(-i\bar{\Omega}\tau)\sum_{n=0}^{\infty}\frac{(-i\tau)^n}{n!}A^n = \exp(-i\bar{\Omega}\tau)(\mathbb{I} - iA\tau), \quad (14)$$

because A^2 vanishes (A is nilpotent). This dynamics is highly reminiscent of the critically damped classical harmonic oscillator, whose time evolution is a superposition of $h_1(t) \simeq \exp(-\gamma t)$ and $h_2(t) \simeq t\exp(-\gamma t)$. Indeed, the critically damped harmonic oscillator formulated as two coupled first-order differential equations results in an EP in the coupling matrix and constitutes a beautiful didactic example for this phenomenon [37]. Equation (14) has several important implications. First, it means that the overall optical power is not conserved when operating at an EP. Instead, the optical amplitudes in general grow linearly, and the optical energy therefore grows quadratically in time. This makes it rather difficult to keep a sensor at an EP for an extended period of time, with dynamics being sensitive to initial excitation conditions [36]. Second, this demonstrates nicely that having a Hamiltonian with only real eigenvalues is not sufficient to ensure energy conservation [38]. To address the former issue, in situations in which high sensitivity is desired, one may encounter a daunting scenario of being in constant need for continuously monitoring and correcting the system so as to bring it back at the EP. In practice, however, this task can be carried out in a considerably less demanding fashion by using the phase transition associated with the EP as a means to eliminate the requirement for constant correction. For example, by modulating the magnitude of the gain around the nominal value for EP and by monitoring the output signal, one can determine the parameter range where the derivative of the response over time reaches its extremum [39,40].

4. DISCUSSION AND CONCLUSION

So far, we have discussed the classical electrodynamics at EPs of $\mathcal{PT}$-symmetric systems, where the spectrum can be real despite the presence of both loss and gain. We have emphasized mesoscopic fluctuations of classical origin, while we speculate that also quantum optics and quantum fluctuations would experience dramatic enhancement near the EP. Indeed, quantum emitter dynamics in the presence of EPs is in itself interesting [31]. In the present context, we note that loss-compensated metamaterials do not necessarily exhibit the dynamics of ideal loss-less structures when probed with quantum optics [41], and as such, there might also be interesting quantum fluctuation properties to be explored in the vicinity of EPs.

Focusing here on the role of mesoscopic fluctuations and noise on the spectral and temporal properties of systems of $\mathcal{PT}$-symmetric coupled gain–loss resonators operating near the EP, we have shown that the inevitable detuning in the frequencies of the uncoupled resonators leads to modified conditions for reaching the EP. In ensembles of resonator pairs, statistical averaging significantly smears the spectral features, which leaves sensitivity of EP-based sensors noise limited. Finally, we have shown how

temporal fluctuations in the detuning and gain of such sensors lead to a quadratic growth of the optical power in time, suggesting that maintaining operation at the EP over a long period might be a formidable task. Since acceptance of this paper, we have become aware of related work in Ref. [42].

REFERENCES

1. B. L. Altshuler, P. A. Lee, and R. A. Webb, eds., *Modern Problems in Condensed Matter Sciences* (Modern Problems in Condensed Matter Sciences, Vol. **30**). (Elsevier, 1991).
2. C. W. J. Beenakker, "Random-matrix theory of quantum transport," Rev. Mod. Phys. **69**, 731–808 (1997).
3. P. W. Anderson, "Absence of diffusion in certain random lattices," Phys. Rev. **109**, 1492–1505 (1958).
4. B. L. Altshuler, D. Khmel'nitzkii, A. I. Larkin, and P. A. Lee, "Magnetoresistance and Hall effect in a disordered two-dimensional electron gas," Phys. Rev. B **22**, 5142–5153 (1980).
5. P. A. Lee and A. D. Stone, "Universal conductance fluctuations in metals," Phys. Rev. Lett. **55**, 1622–1625 (1985).
6. B. N. Narozhny and I. L. Aleiner, "Mesoscopic fluctuations of the coulomb drag," Phys. Rev. Lett. **84**, 5383–5386 (2000).
7. N. A. Mortensen, K. Flensberg, and A.-P. Jauho, "Coulomb drag in coherent mesoscopic systems," Phys. Rev. Lett. **86**, 1841–1844 (2001).
8. A. M. Lunde, K. Flensberg, and L. I. Glazman, "Interaction-induced resonance in conductance and thermopower of quantum wires," Phys. Rev. Lett. **97**, 256802 (2006).
9. M. C. Goorden and M. Büttiker, "Two-particle scattering matrix of two interacting mesoscopic conductors," Phys. Rev. Lett. **99**, 146801 (2007).
10. N. M. Lawandy, R. M. Balachandran, A. S. L. Gomes, and E. Sauvain, "Laser action in strongly scattering media," Nature **368**, 436–438 (1994).
11. J. R. Ott, N. A. Mortensen, and P. Lodahl, "Quantum interference and entanglement induced by multiple scattering of light," Phys. Rev. Lett. **105**, 090501 (2010).
12. L. Sapienza, H. Thyrrestrup, S. Stobbe, P. D. Garcia, S. Smolka, and P. Lodahl, "Cavity quantum electrodynamics with Anderson-localized modes," Science **327**, 1352–1355 (2010).
13. J. Liu, P. D. Garcia, S. Ek, N. Gregersen, T. Suhr, M. Schubert, J. Mørk, S. Stobbe, and P. Lodahl, "Random nanolasing in the Anderson localized regime," Nat. Nanotechnol. **9**, 285–289 (2014).
14. S. Datta, *Electronic Transport in Mesoscopic Systems* (Cambridge University, 1995).
15. S. H. Fan, W. Suh, and J. D. Joannopoulos, "Temporal coupled-mode theory for the fano resonance in optical resonators," J. Opt. Soc. Am. A **20**, 569–572 (2003).
16. A. Yariv, Y. Xu, R. K. Lee, and A. Scherer, "Coupled-resonator optical waveguide: a proposal and analysis," Opt. Lett. **24**, 711–713 (1999).
17. J. Grgić, J. R. Ott, F. Wang, O. Sigmund, A.-P. Jauho, J. Mørk, and N. A. Mortensen, "Fundamental limitations to gain enhancement in periodic media and waveguides," Phys. Rev. Lett. **108**, 183903 (2012).
18. J. Grgić, E. Campaioli, S. Raza, P. Bassi, and N. A. Mortensen, "Coupled-resonator optical waveguides: Q-factor and disorder influence," Opt. Quantum Electron. **42**, 511–519 (2011).
19. S. Xiao, V. P. Drachev, A. V. Kildishev, X. Ni, U. K. Chettiar, H.-K. Yuan, and V. M. Shalaev, "Loss-free and active optical negative-index metamaterials," Nature **466**, 735–738 (2010).
20. R. El-Ganainy, K. G. Makris, M. Khajavikhan, Z. H. Musslimani, S. Rotter, and D. N. Christodoulides, "Non-Hermitian physics and PT symmetry," Nat. Phys. **14**, 11–19 (2018).
21. S. Longhi, "Parity-time symmetry meets photonics: a new twist in non-Hermitian optics," Europhys. Lett. **120**, 64001 (2017).
22. C. M. Bender and S. Boettcher, "Real spectra in non-Hermitian Hamiltonians having PT symmetry," Phys. Rev. Lett. **80**, 5243–5246 (1998).
23. A. Guo, G. J. Salamo, D. Duchesne, R. Morandotti, M. Volatier-Ravat, V. Aimez, G. A. Siviloglou, and D. N. Christodoulides, "Observation of PT-symmetry breaking in complex optical potentials," Phys. Rev. Lett. **103**, 093902 (2009).
24. C. E. Rüter, K. G. Makris, R. El-Ganainy, D. N. Christodoulides, M. Segev, and D. Kip, "Observation of parity-time symmetry in optics," Nat. Phys. **6**, 192–195 (2010).
25. A. Regensburger, C. Bersch, M.-A. Miri, G. Onishchukov, D. N. Christodoulides, and U. Peschel, "Parity-time synthetic photonic lattices," Nature **488**, 167–171 (2012).
26. M. Brandstetter, M. Liertzer, C. Deutsch, P. Klang, J. Schöberl, H. E. Türeci, G. Strasser, K. Unterrainer, and S. Rotter, "Reversing the pump dependence of a laser at an exceptional point," Nat. Commun. **5**, 4034 (2014).
27. B. Peng, S. K. Özdemir, F. Lei, F. Monifi, M. Gianfreda, G. L. Long, S. Fan, F. Nori, C. M. Bender, and L. Yang, "Parity-time-symmetric whispering-gallery microcavities," Nat. Phys. **10**, 394–398 (2014).
28. H. Hodaei, M.-A. Miri, M. Heinrich, D. N. Christodoulides, and M. Khajavikhan, "Parity-time-symmetric microring lasers," Science **346**, 975–978 (2014).
29. Z. Gao, S. Fryslie, B. Thompson, P. Carney, and K. Choquette, "Parity-time symmetry in coherently coupled vertical cavity laser arrays," Optica **4**, 323–329 (2017).
30. J. Miller, "Exceptional points make for exceptional sensors," Phys. Today **70**(10), 23–26 (2017).
31. A. Pick, B. Zhen, O. D. Miller, C. W. Hsu, F. Hernandez, A. W. Rodriguez, M. Soljačić, and S. G. Johnson, "General theory of spontaneous emission near exceptional points," Opt. Express **25**, 12325–12348 (2017).
32. J. Wiersig, "Enhancing the sensitivity of frequency and energy splitting detection by using exceptional points: application to microcavity sensors for single-particle detection," Phys. Rev. Lett. **112**, 203901 (2014).
33. H. Hodaei, A. U. Hassan, S. Wittek, H. Garcia-Gracia, R. El-Ganainy, D. N. Christodoulides, and M. Khajavikhan, "Enhanced sensitivity at higher-order exceptional points," Nature **548**, 187–191 (2017).
34. M. Svedendahl, S. Chen, A. Dmitriev, and M. Käll, "Refractometric sensing using propagating versus localized surface plasmons: a direct comparison," Nano Lett. **9**, 4428–4433 (2009).
35. R. Ameling and H. Giessen, "Microcavity plasmonics: strong coupling of photonic cavities and plasmons," Laser Photon. Rev. **7**, 141–169 (2013).
36. S. Longhi, "Exceptional points and photonic catastrophe," Opt. Lett. **43**, 2929–2932 (2018).
37. G. Dolfo and J. Vigué, "Damping of coupled harmonic oscillators," Eur. J. Phys. **39**, 025005 (2018).
38. C. M. Bender, "Making sense of non-Hermitian Hamiltonians," Rep. Prog. Phys. **70**, 947–1018 (2007).
39. J. Ren, H. Hodaei, G. Harari, A. U. Hassan, W. Chow, M. Soltani, D. Christodoulides, and M. Khajavikhan, "Ultrasensitive micro-scale parity-time-symmetric ring laser gyroscope," Opt. Lett. **42**, 1556–1559 (2017).
40. W. Chen, S. K. Özdemir, G. Zhao, J. Wiersig, and L. Yang, "Exceptional points enhance sensing in an optical microcavity," Nature **548**, 192–196 (2017).
41. E. Amooghorban, N. A. Mortensen, and M. Wubs, "Quantum optical effective-medium theory for loss-compensated metamaterials," Phys. Rev. Lett. **110**, 153602 (2013).
42. W. Langbein, "No exceptional precision of exceptional-point sensors," Phys. Rev. A **98**, 023805 (2018).